JCB Article

The fission yeast cytokinesis formin Cdc12p is a barbed end actin filament capping protein gated by profilin

David R. Kovar, Jeffrey R. Kuhn, Andrea L. Tichy, and Thomas D. Pollard

Department of Molecular, Cellular, and Developmental Biology, Yale University, New Haven, CT 06520

Cytokinesis in most eukaryotes requires the assembly and contraction of a ring of actin filaments and myosin II. The fission yeast *Schizosaccharomyces pombe* requires the formin Cdc12p and profilin (Cdc3p) early in the assembly of the contractile ring. The proline-rich formin homology (FH) 1 domain binds profilin, and the FH2 domain binds actin. Expression of a construct consisting of the Cdc12 FH1 and FH2 domains complements a conditional mutant of Cdc12 at the restrictive temperature, but arrests cells at the permissive temperature. Cells overexpressing Cdc12(FH1FH2)p stop growing with excessive actin cables but no contractile rings. Like capping protein, purified Cdc12(FH1FH2)p caps the barbed end of actin filaments, preventing subunit addition and dissociation, inhibits end to end annealing of filaments, and nucleates filaments that grow exclusively from their pointed ends. The maximum yield is one filament pointed end per six formin polypeptides. Profilins that bind both actin and poly-L-proline inhibit nucleation by Cdc12(FH1FH2)p, but polymerization of monomeric actin is faster, because the filaments grow from their barbed ends at the same rate as uncapped filaments. On the other hand, Cdc12(FH1FH2)p blocks annealing even in the presence of profilin. Thus, formins are profilin-gated barbed end capping proteins with the ability to initiate actin filaments from actin monomers bound to profilin. These properties explain why contractile ring assembly requires both formin and profilin and why viability depends on the ability of profilin to bind both actin and poly-L-proline.

Introduction

Compared with the rapidly accumulating evidence about the assembly of the actin network at the leading edge of cells (Pollard and Borisy, 2003), much less is known about the assembly of the actomyosin contractile ring during cytokinesis (Robinson and Spudich, 2000). Lacking biochemical assays for cytokinesis, the field has depended largely on genetics to identify the participating proteins. The fission yeast *Schizosaccharomyces pombe* is the cell with the most complete inventory of cytokinesis genes, >50 (Le Goff et al., 1999; Guertin et al., 2002). Both preexisting and newly polymerized actin filaments contribute to the contractile ring, which turns over throughout cleavage (Pelham and Chang, 2002). Actin-binding proteins that coordinate contractile ring assembly in fission yeast include IQGAP (Rng2p), type-II myosins (Myo2p and Myp2p), Arp2/3 complex (arp3 and wsp1), tropomyosin (Cdc8p), profilin (Cdc3p), and the formin Cdc12p (for reviews see Le Goff et al., 1999; Feierbach and Chang, 2001a; Guertin et al., 2002).

Formins, cytoskeleton-organizing proteins of plants, animals, and fungi, contain three conserved formin homology (FH)* domains: FH1, FH2, and FH3 (for review see Wasserman, 1998). FH1 is rich in proline and binds profilin (Wasserman, 1998), and FH2 interacts with actin (Pruyne et al., 2002; Pring et al., 2003). Other domains are responsible for localization, autoinhibition, and regulation by Rho-family GTPases (Alberts, 2001). Fission yeast has three formin genes: *cdc12*, required for cytokinesis (Chang et al., 1997), *for3*, required for interphase actin cables (Feierbach and Chang, 2001b; Nakano et al., 2002), and *fus1*, required for mating (Petersen et al., 1998).

The online version of this article includes supplemental material.

Address correspondence to Thomas D. Pollard, MCDB, KBT-548, Yale University, P.O. Box 208103, New Haven, CT 06520-8103. Tel.: (203) 432-3460. Fax: (203) 432-6161. E-mail: thomas.pollard@yale.edu

Key words: actin cables; annealing; capping protein; contractile ring; *S. pombe*

*Abbreviations used in this paper: FH, formin homology; *Mm*CP, *Mus musculus* capping protein; TIRF, total internal reflection fluorescence.

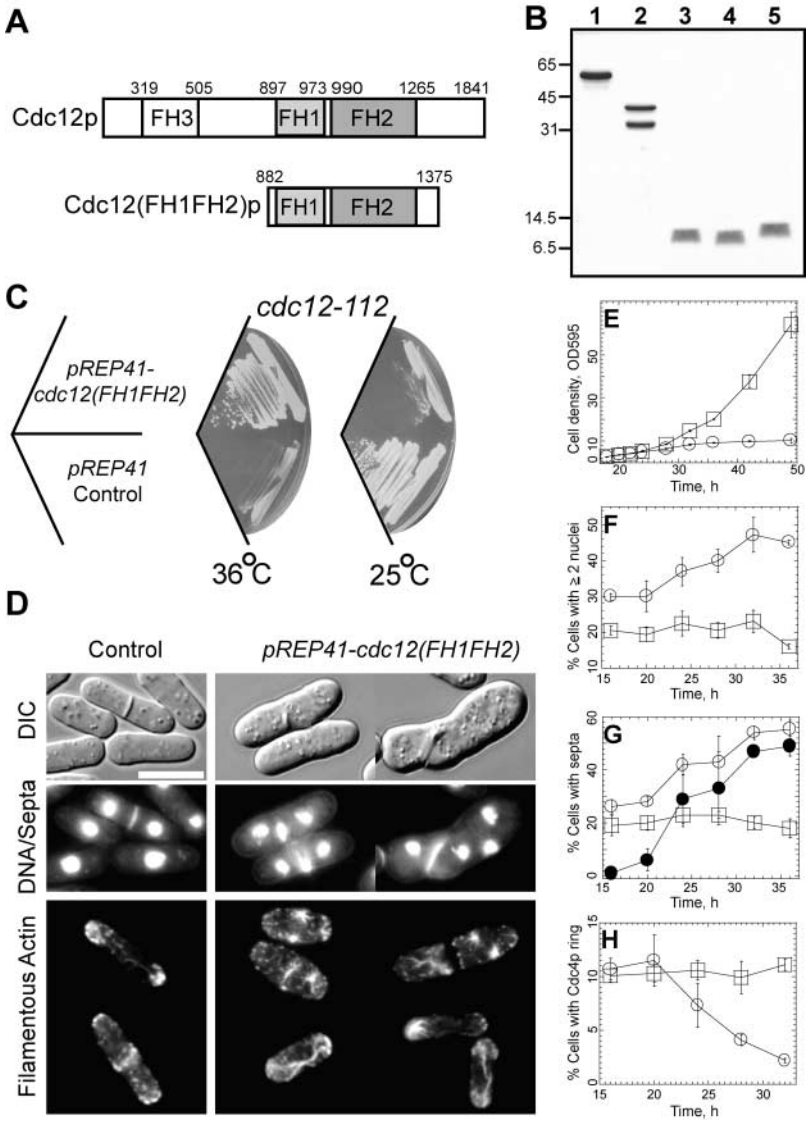

Figure 1. **Fission yeast formin Cdc12 domains, purified protein, complementation of a temperature-sensitive *cdc12* mutant, and overexpression of Cdc12(FH1FH2)p in wild-type cells.** (A) Domain organization of Cdc12p and the Cdc12(FH1FH2)p construct. (B) Purified proteins separated by SDS-PAGE and stained with Coomassie blue; (lane 1) Cdc12(FH1FH2)p, (lane 2) mouse capping protein *Mm*CP, (lane 3) wild-type fission yeast profilin *Sp*PRF, (lane 4) profilin mutant *Sp*PRF-K81E, (lane 5) profilin mutant *Sp*PRF-Y5D. Molecular weights are indicated on the left. (C) The formin fragment Cdc12(FH1FH2)p complements a temperature-sensitive *cdc12* mutant (*cdc12-112*). *Cdc12-112* cells with either a control (*pREP41*) or a *pREP41-cdc12(FH1FH2)* plasmid were grown in the absence of thiamine to induce expression of Cdc12(FH1FH2)p. Overexpression of Cdc12(FH1FH2)p allowed growth of *cdc12-112* cells at the restrictive temperature (36°C) but arrested cells at the permissive temperature (25°C) on minimal media (EMM) plates after 72 h. (D–H) Overexpression of Cdc12(FH1FH2)p in wild-type cells. Wild-type cells with either a control (*pREP41*) or a *pREP41-cdc12(FH1FH2)* plasmid were grown in the absence of thiamine to induce expression of Cdc12(FH1FH2)p. (D) Differential interference contrast (DIC) and fluorescence micrographs of control cells and cells overexpressing Cdc12(FH1FH2)p for 24 h at 25°C in minimal (EMM) liquid media. Cells were stained for nuclei and septa (Hoechst) or filamentous actin (rhodamine-phalloidin). Cells overexpressing Cdc12(FH1FH2)p had multiple nuclei, partial and misoriented septa, and increased actin aggregates and cables, but lack actin patches and contractile rings. Bar, 5 μm. (E–H) Quantitation of the time course of morphological features of cells with a (□) *pREP41* control plasmid or a (○) *pREP41-cdc12(FH1FH2)* plasmid overexpressing Cdc12(FH1FH2)p by removal of thiamine at time zero. (E) Cell density (OD_{595}). (F) Percent of cells with multiple nuclei. (G) Percent of cells with normal septa and (●) abnormal septa for *pREP41-cdc12(FH1FH2)*. (H) Percent of cells with contractile rings marked with a myosin essential light chain (GFP–Cdc4p).

Many formins participate in cytokinesis, and some localize to the cleavage furrow (Pelham and Chang, 2002; Severson et al., 2002; Tolliday et al., 2002; for reviews see Frazier and Field, 1997; Wasserman, 1998). Both formin and the small actin–binding protein profilin (Balasubramanian et al., 1994; Haugwitz et al., 1994; Verheyen and Cooley, 1994; Severson et al., 2002; Tolliday et al., 2002) are required for cytokinesis and incorporation of actin into the contractile ring (Pelham and Chang, 2002; Tolliday et al., 2002). Formins appear to act directly on actin, because expression of a fragment of the budding yeast formins Bni1p and Bnr1p, containing the FH1 and FH2 domains, induces actin cables in vivo (Evangelista et al., 2002; Sagot et al., 2002a), and because isolated Bni(FH1FH2)p stimulates the polymerization of purified actin (Pruyne et al., 2002; Sagot et al., 2002b; Pring et al., 2003). Interestingly, profilin is required for formin to promote actin assembly in vivo (Evangelista et al., 2002; Sagot et al., 2002a) but not in vitro (Pruyne et al., 2002; Sagot et al., 2002b; Pring et al., 2003).

To learn why contractile ring assembly in fission yeast depends on both the formin Cdc12p and the profilin Cdc3p, we characterized the FH1 and FH2 domains of Cdc12p, which correspond to the domains of Bni1p that stimulate actin assembly. In the absence of profilin, formins nucleate actin assembly similar to capping proteins (Cooper and Pollard, 1985), but profilin changes the mechanism so that Cdc12(FH1FH2)p nucleates filaments that grow rapidly from their barbed ends. These results explain why cells depend on both formin and profilin for actin polymerization during contractile ring assembly in vivo.

Results

Overexpression of formin Cdc12(FH1FH2)p in fission yeast

To learn how the fission yeast formin Cdc12p regulates actin filament assembly during cytokinesis, we focused on a construct consisting of the FH1 and FH2 domains (Fig. 1

A; Cdc12(FH1FH2)p). Although this fragment lacks the regulatory domains flanking the FH1 and FH2 domains, the comparable fragment of the budding yeast formin Bni1p promotes actin polymerization in vivo and in vitro (Evangelista et al., 2002; Pruyne et al., 2002; Sagot et al., 2002a,b). The size of the Cdc12(FH1FH2)p fragment is based upon the Bni1(FH1FH2)p fragment of Sagot et al. (2002b), which is shorter by ~70 residues than the Bni1(FH1FH2)p fragment of Pruyne et al. (2002) and Pring et al. (2003) at the COOH terminus of the FH2 domain. Cdc12 (FH1FH2)p is a functional fragment, as overexpression of Cdc12(FH1FH2)p complemented the *cdc12-112* temperature-sensitive mutant (Chang et al., 1997) at the restrictive temperature of 36°C (Fig. 1 C). Overexpression of Cdc12 (FH1FH2)p arrested the growth of both *cdc12-112* cells at the permissive temperature of 25°C (Fig. 1 C) and wild-type cells (Fig. 1, D–H). Thus, Cdc12(FH1FH2)p can replace the essential functions of Cdc12p in vivo when Cdc12p is nonfunctional, but is toxic when overexpressed in the presence of functional Cdc12p.

Wild-type fission yeast overexpressing Cdc12(FH1FH2)p contained an impressive enrichment of actin filaments in aberrant thick cables and aster-like accumulations when visualized with rhodamine-phalloidin, but lacked both actin contractile rings and polarized actin patches (Fig. 1 D). Cells overexpressing Cdc12(FH1FH2)p arrested after ~24 h (Fig. 1 E). Growth arrest coincided with an increase in cells with multiple nuclei (Fig. 1 F) and abnormal (partial, broad, and misoriented) septa (Fig. 1 G) and a decrease in cells with contractile rings (Fig. 1 H).

Effects of Cdc12(FH1FH2)p on subunit association and dissociation at the ends of actin filaments

Like budding yeast Bni1(FH1FH2)p, fission yeast Cdc12 (FH1FH2)p purified from bacteria (Fig. 1 B) stimulated actin polymerization, as detailed below (see Fig. 4). Interpretation of these experiments requires knowledge of the effect of these constructs on the addition and dissociation of subunits at the two ends of the filaments. Therefore, we begin with three independent lines of evidence that Cdc12(FH1FH2)p caps the barbed ends of actin filaments with high affinity, allowing elongation only at pointed ends.

First, 100 nM Cdc12(FH1FH2)p increased the critical concentration (C_c) for actin assembly from 0.13 μM, near the critical concentration of the barbed end, to 0.9 μM, the critical concentration of the pointed end (Fig. 2 A). 10 nM *Mus musculus* capping protein (*Mm*CP; Palmgren et al., 2001) shifted the critical concentration to 1.0 μM (Fig. 2 A). The critical concentration depended on the concentration of Cdc12(FH1FH2)p (Fig. 2 B), with the shift from the barbed to pointed end occurring between 1 and 10 nM Cdc12(FH1FH2)p. Thus, the dissociation equilibrium constant (K_d) for Cdc12(FH1FH2)p at barbed ends is <0.5 μM (Caldwell et al., 1989).

Second, both Cdc12(FH1FH2)p and *Mm*CP inhibited depolymerization of actin filaments diluted to 0.1 μM (Fig. 2 C). Cdc12(FH1FH2)p reduced the rate of depolymerization to 34% of the rate in the absence of formin (Fig. 2 D). *Mm*CP reduced the rate of depolymerization to 27% (Fig. 2 D). This is consistent with Cdc12(FH1FH2)p and *Mm*CP

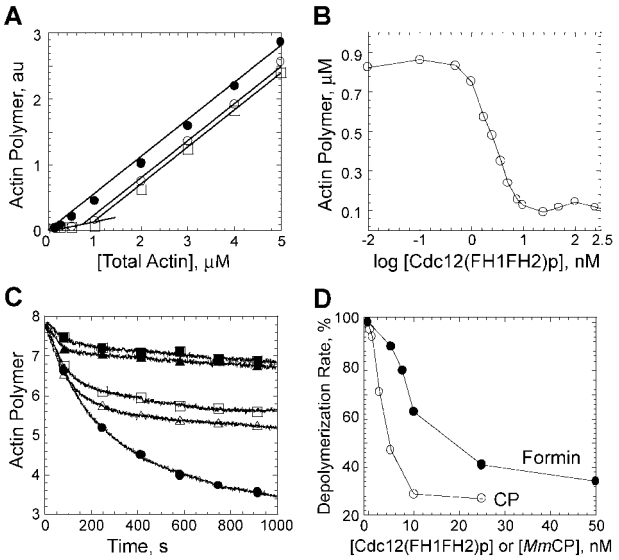

Figure 2. **Effect of Cdc12(FH1FH2)p and mouse capping protein (*Mm*CP) on actin depolymerization and critical concentration.** The conditions were as follows: 10 mM imidazole, pH 7.0, 50 mM KCl, 1 mM $MgCl_2$, 1 mM EGTA, 0.5 mM DTT, 0.2 mM ATP, 90 μM $CaCl_2$, and 0.25% glycerol at 25°C. (A and B) Critical concentration for assembly of rabbit skeletal muscle actin. (A) Dependence of actin polymer concentration on total actin concentration in the (●) absence or presence of either (□) 10 nM *Mm*CP or (○) 100 nM Cdc12(FH1FH2)p. Actin (5% pyrene labeled) was polymerized for 16 h. The polymer concentration was measured from the pyrene fluorescence, plotted versus actin concentration, and fit by linear regression. The C_c values were 0.1 μM for actin alone, 0.9 μM with 100 nM Cdc12(FH1FH2)p, and 1.0 μM with 10 nM *Mm*CP. (B) Dependence of the polymer concentration of 1 μM actin on the concentration of Cdc12(FH1FH2)p. 5 μM actin filaments (10% pyrene labeled) were diluted to 1 μM in the presence of a range of Cdc12(FH1FH2)p concentrations. After 16 h, the pyrene fluorescence was measured, and the actin polymer concentration was plotted versus the log of Cdc12(FH1FH2)p concentration. (C and D) Time course of depolymerization of 5 μM actin filaments (70% pyrene labeled) after dilution to 0.1 μM in the presence of a range of concentrations of Cdc12(FH1FH2)p, (●) 0, (△) 7.5 nM, and (▲) 25 nM, or a range of concentrations of *Mm*CP, (●) 0, (□) 2.5 nM, and (■) 10 nM. (D) Dependence of the rate of depolymerization on the concentration of (●) Cdc12(FH1FH2)p or (○) *Mm*CP. The data from 300–1,000 s of each curve was fit with single exponentials, and the depolymerization rates were expressed as a fraction of the rate of actin alone.

capping the barbed (fast depolymerizing) ends of the filaments with high affinity (K_d < 0.1 μM), allowing dissociation only from the slowly depolymerizing (Pollard, 1986) pointed ends (Caldwell et al., 1989). In both cases, an initial fast phase of depolymerization was followed by a slow phase, as expected for a second order barbed end capping reaction.

Third, real-time visualization of actin assembly by total internal reflection fluorescence (TIRF) microscopy (Amann and Pollard, 2001) revealed that Cdc12(FH1FH2)p caps barbed ends but allows growth at pointed ends (Fig. 3). Actin alone elongated at both ends: 19 subunits/s at the barbed ends and 0.8 subunits/s at the pointed ends (Fig. 3 A). These rates are slightly slower than expected from the established rate constants (Pollard, 1986) because elongation of labeled actin is slower than unlabeled actin (Amann and Pollard, 2001; unpublished data). After 500 s, the filaments

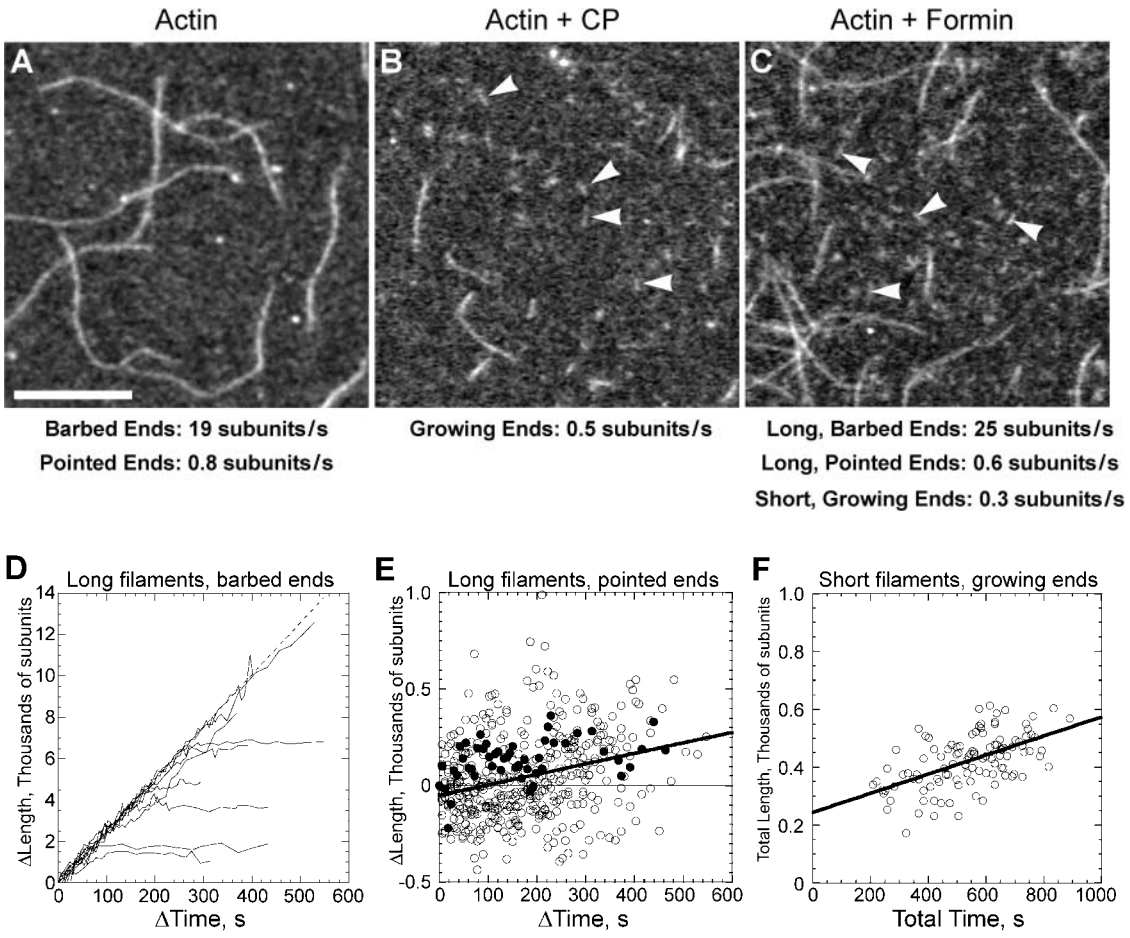

Figure 3. **Real-time visualization of actin assembly in the presence of Cdc12(FH1FH2)p or mouse capping protein by TIRF microscopy.** The conditions were as follows: 3 μM (25% Oregon green 488–labeled) Mg-ATP actin, 10 mM imidazole, pH 7.0, 50 mM KCl, 1 mM $MgCl_2$, 1 mM EGTA, 50 mM DTT, 0.2 mM ATP, 50 μM $CaCl_2$, 15 mM glucose, 20 μg/ml catalase, 100 μg/ml glucose oxidase, 0.5% methylcellulose at 25°C. Flow cells were coated with NEM-myosin to capture the actin filaments. Direct comparisons of samples stained with rhodamine-phalloidin and adsorbed to coverslips coated with poly-L-lysine (Fig. 4) showed that the conditions of these TIRF experiments strongly favored the observation of long filaments. In fact, we observed no filaments at concentrations of Cdc12(FH1FH2)p >500 nM, where the biochemical results (and rhodamine-phalloidin staining) indicated numerous short filaments. (A–C) Images of actin filaments 500 s after initiating the reactions. Bar, 10 μm or 3,700 subunits. (A) Actin alone. (B) Actin with 50 nM *Mm*CP. Both long filaments (n = 15) and short filaments (n = 12; arrowheads) grew at a pointed end rate of 0.5 ± 0.1 subunits/s. (C) Actin with 250 nM Cdc12(FH1FH2)p. (D–F) Measurements of changes in filament length with time. Control filament barbed ends grew at 19.0 ± 0.1 subunits/s (n = 16 filaments), and pointed ends grew at 0.8 ± 0.1 subunits/s (n = 16). (D) Barbed ends in the presence of Cdc12(FH1FH2)p. The longer filaments (dashed line) grew at 25.2 ± 0.2 subunits/s (n = 10) until they stopped abruptly at random times. (E) Pointed ends of long filaments in the presence of Cdc12(FH1FH2)p grew continuously (solid line) at a rate of 0.6 ± 0.1 subunits/s (n = 10). Measurements from a single filament are indicated by filled circles. (F) Short filaments in the presence of Cdc12(FH1FH2)p. The total length of short filaments (arrowheads in C) versus total reaction time showed uniform growth at a rate of 0.3 ± 0.1 subunits/s (solid line; n = 10) and an apparent starting length of 240 ± 30 subunits. Diffraction increased the apparent 1/e width and length of individual actin filaments to 0.7 μm, or 260 subunits, so the starting length was zero.

ranged in length from <500 to >10,000 subunits, as appropriate for a population that formed at random times by spontaneous nucleation and grew at 20 subunits/s for up to 500 s.

Mouse capping protein produced two populations of filaments: many with short, uniform lengths and others with intermediate but variable lengths (Fig. 3 B). All of these filaments grew at only one end, at a rate of 0.5 subunits/s, as appropriate for pointed ends. Given their length and the time available for polymerization, the few filaments of intermediate length must have formed spontaneously and grown transiently at their barbed ends before being capped. These events occurred during the 90 s required to prepare these samples. In other experiments, the addition of capping protein to elongating actin filaments in a flow cell abruptly stopped barbed end growth (unpublished data).

The polymerization of actin in the presence of Cdc12 (FH1FH2)p produced numerous short filaments and some longer filaments (Fig. 3 C). The population of short, uniform filaments grew at a rate of 0.3 subunits/s, consistent with growing from only the pointed end. Robust linear regression of a plot of total length versus reaction time (Fig. 3 F) placed the apparent starting length of the short filaments at 240 subunits. As all dimensions of these filaments are inflated by ~260 subunits (measured from the width of the fluorescent images), these short filaments were initiated soon after mixing Cdc12(FH1FH2)p with actin and therefore were nucleated by Cdc12(FH1FH2)p. The population of

longer actin filaments initially grew at both ends, accounting for their considerable lengths. Fast ends grew at a barbed end rate of 25 subunits/s until they stopped permanently at random times (Fig. 3 D). These capping events occurred over a much longer time than capping by *Mm*CP, so we conclude that *Mm*CP caps barbed ends faster than Cdc12 (FH1FH2)p. The slower ends of the long filaments grew at a pointed end rate of 0.6 subunits/s throughout the time course (Fig. 3 E). This rate was slightly higher than the polymerization rate of the short filaments, but the difference is not significant given the noise in these assays.

Effect of Cdc12(FH1FH2)p on spontaneous actin assembly

Fission yeast Cdc12(FH1FH2)p stimulated the spontaneous assembly of Mg-actin monomers, reducing the lag at the onset of the reaction and increasing the maximum rate of polymerization just like *Mm*CP (Fig. 4 A). The stimulation of polymerization depended on the concentration of each protein (Fig. 4 B) and the effects of Cdc12(FH1FH2)p and *Mm*CP were additive (Fig. 4 C) rather than antagonistic. Both Cdc12(FH1FH2)p and *Mm*CP required almost 2.0 μM Mg–G-actin to stimulate spontaneous polymerization (Fig. 4 H).

Fluorescence microscopy of the products of these reactions labeled with rhodamine-phalloidin showed that filaments formed in the presence of either *Mm*CP (Fig. 4 F) or Cdc12(FH1FH2)p (Fig. 4 G) were much shorter than actin alone (Fig. 4 E). Number average filament lengths depended on the concentration of Cdc12(FH1FH2)p: 20 μm for 4 μM Mg-ATP actin alone; 1.8 μm in 25 nM Cdc12 (FH1FH2)p; 1.02 μm in 100 nM; 0.8 μm for 200 nM; and 0.6 μm in 250 nM. The average length was 0.9 μm in 100 nM *Mm*CP. Thus, formin and capping protein nucleated numerous filaments that grew slowly and did not anneal.

Knowing that filaments grow at their pointed ends, we calculated that Cdc12(FH1FH2)p produced a maximum concentration of ~17 nM ends (Fig. 4 B). The maximum yield of 0.17 pointed ends per formin polypeptide was at 5.0 nM Cdc12(FH1FH2)p (Fig. 4 D), with lower yields at higher concentrations (Fig. 4 D). *Mm*CP also produced a maximum of 17 nM pointed ends (Fig. 4 B), with a maximum yield of 0.29 filaments per capping protein heterodimer at 10 nM *Mm*CP (Fig. 4 D). A nucleation efficiency of <100%, which peaks at a low concentration of barbed end capper, is expected from the strong actin monomer concentration dependence of nucleation (Fig. 4 H) and the depletion of the subunit pool by the high concentration of pointed ends, which consume subunits faster than the rate of nucleation.

Effect of profilin and Cdc12(FH1FH2)p on actin filament elongation

Profilin had a dramatic influence on Cdc12(FH1FH2)p, inhibiting nucleation but allowing full-speed growth at barbed ends. The net effect of profilin is the assembly of fewer filaments that grow rapidly at their barbed ends. We will present the case for this mechanism starting with the evidence for barbed end growth.

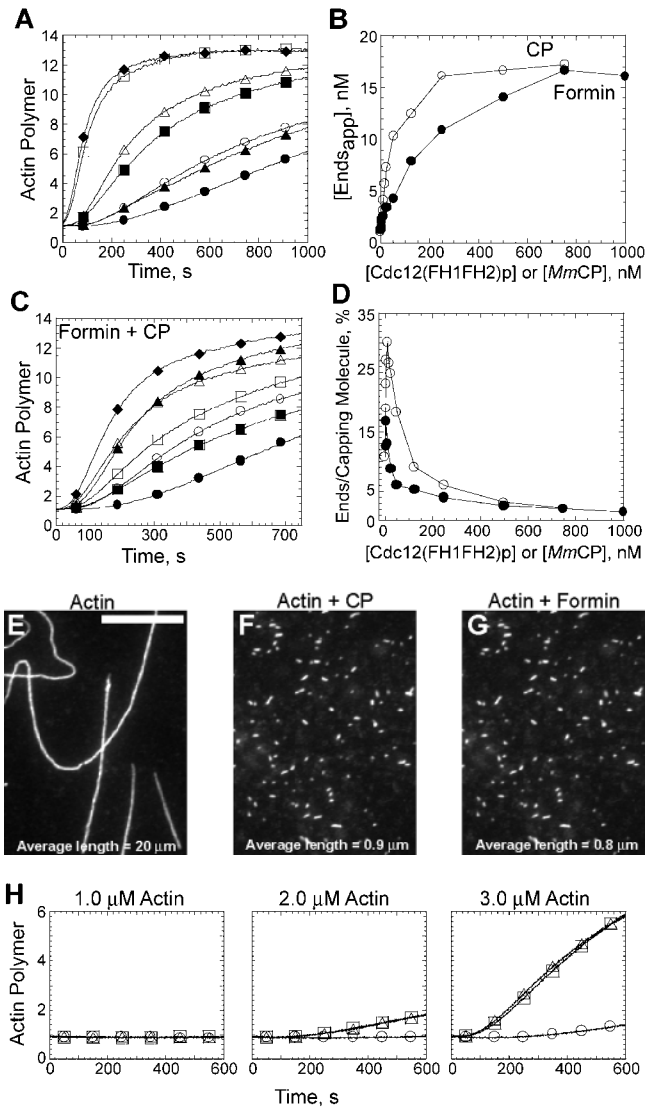

Figure 4. **Effects of Cdc12(FH1FH2)p and mouse capping protein on spontaneous polymerization of Mg-ATP muscle actin.** The buffer used was the same as in Fig. 2. (A and B) The time course of the polymerization of 4 μM Mg-ATP actin (5% pyrene labeled) was monitored by fluorescence in the presence of a range of concentrations of Cdc12(FH1FH2)p, (●) 0, (○) 5 nM, (■) 25 nM, and (□) 500 nM, or a range of concentrations (nM) of *Mm*CP, (●) 0, (▲) 2.5 nM, (△) 17.5 nM, and (◆) 250 nM. (B) Dependence of the concentration of apparent pointed ends ([Ends$_{app}$], nM) on the concentration of (●) Cdc12(FH1FH2)p or (○) *Mm*CP calculated from the rate of polymerization at the time where 40% (1.6 μM) of the actin was polymerized. (C) Effect of mixtures of Cdc12(FH1FH2)p and *Mm*CP on the time course of actin assembly; (●) 4 μM actin alone or 4 μM actin with (○) 10 nM Cdc12(FH1FH2)p, (■) 4 nM *Mm*CP, (□) 10 nM Cdc12(FH1FH2)p + 4 nM *Mm*CP, (▲) 50 nM Cdc12(FH1FH2)p, (△) 17 nM *Mm*CP, or (◆) 50 nM Cdc12(FH1FH2)p + 17 nM *Mm*CP. (D) Yield of [Ends$_{app}$] (calculated from B) per capping molecule as a function of the concentration of (●) Cdc12(FH1FH2)p or (○) *Mm*CP. (E–G) Fluorescence micrographs of filaments assembled to steady state from actin alone or with Cdc12(FH1FH2)p or *Mm*CP. Samples were labeled with rhodamine-phalloidin and adsorbed to glass coverslips coated with poly-L-lysine to capture short filaments (~0.1–0.5 μm), but many more short filaments were free in solution. Bar, 10 μm. (E) 4 μM Mg-ATP actin assembled alone for 45 min. (F) Actin assembled with 100 nM *Mm*CP for 10 min. (G) Actin assembled with 200 nM Cdc12(FH1FH2)p for 10 min. (H) Time course of polymerization of the indicated concentrations of Mg-ATP actin alone (○) or with (□) 100 nM Cdc12(FH1FH2)p or (△) 25 nM *Mm*CP.

Direct visualization by TIRF microscopy confirmed earlier evidence (Pollard and Cooper, 1984; Kaiser et al., 1999; Kang et al., 1999; Kinosian et al., 2002) that profilin inhibits elongation by Mg-ATP actin at filament pointed ends but not at barbed ends (Fig. 5, compare D and E with F and G). However, more striking was the finding that profilin reversed the polarity of actin filament elongation in the presence of Cdc12(FH1FH2)p. Instead of growing only at their pointed ends as with Cdc12(FH1FH2)p alone, all of the filaments measured (chosen randomly) with both Cdc12

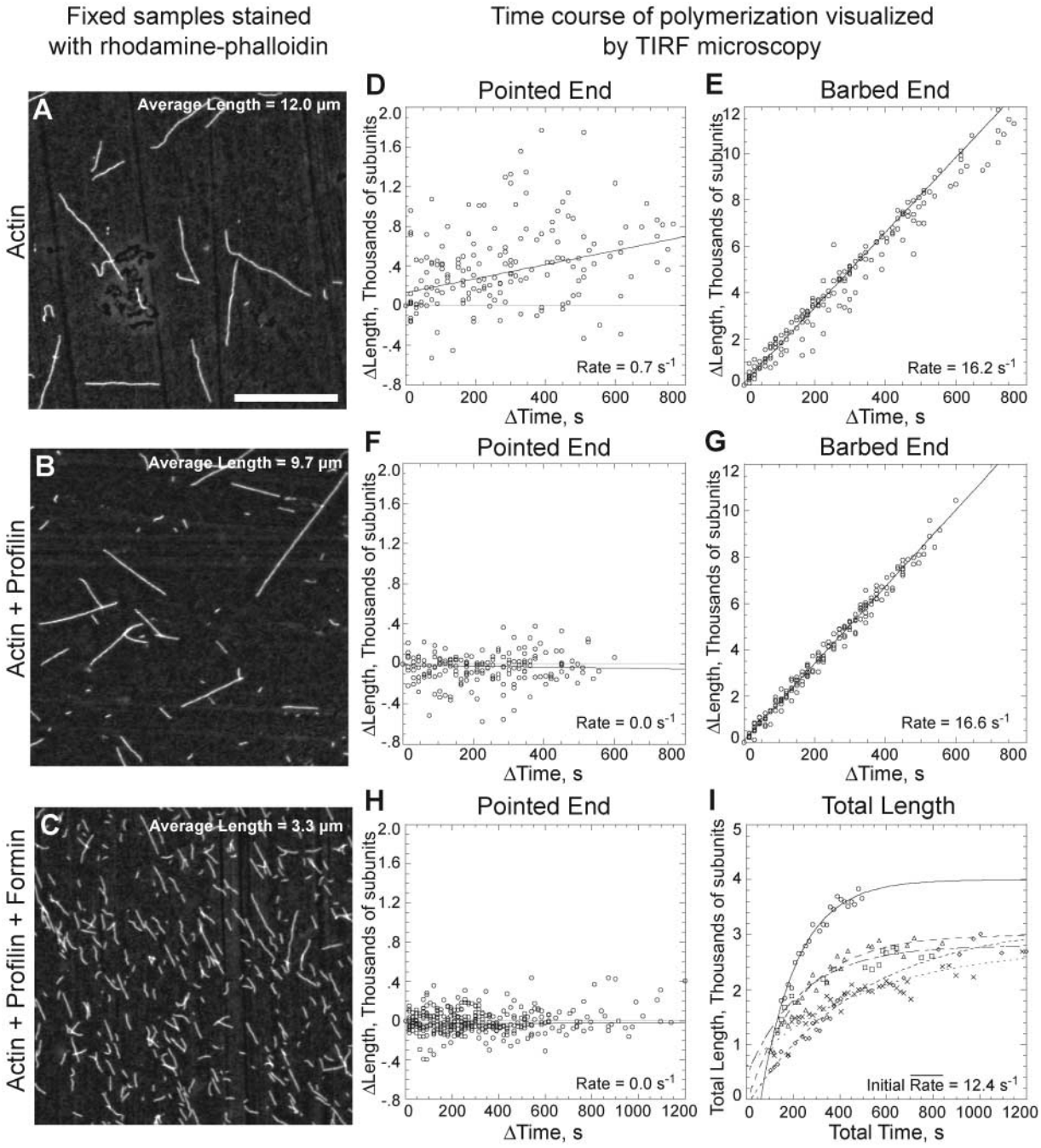

Figure 5. **Visualization of actin filament elongation in the presence of profilin and Cdc12(FH1FH2)p.** The buffer used was the same as in Fig. 3. (A–C) Fixed samples from TIRF microscopy reactions were labeled with rhodamine-phalloidin 15 min after the reaction start, diluted 1:59, and adsorbed to glass coverslips coated with poly-L-lysine. (A) 3 μM actin alone. (B) Actin plus 5 μM profilin. (C) Actin plus 100 nM Cdc12(FH1FH2)p and 5 μM profilin. Bar, 10 μm or 3,700 subunits. (D–I) Growth of individual actin filament ends was observed with TIRF microscopy. For actin alone, (D) pointed ends grew at 0.7 ± 0.1 subunits/s (n = 10) and (E) barbed ends grew at 16.2 ± 0.1 subunits/s (n = 10). In the presence of 5 μM profilin, (F) pointed end growth was inhibited to 0.0 ± 0.1 subunits/s (n = 11), whereas (G) barbed ends grew at 16.6 ± 0.1 subunits/s (n = 11). In the presence of 5 μM profilin and 100 nM Cdc12(FH1FH2)p, (H) pointed end growth was inhibited to 0.00 ± 0.03 subunits/s (n = 13), (I) whereas barbed ends grew at an initial rate of 12.4 ± 5.9 subunits/s (n = 12) before the free actin subunit pool was depleted. (I) The total length over time for each filament was fitted to an exponential growth curve to estimate the initial growth rate and nucleation time. Five example filaments are shown.

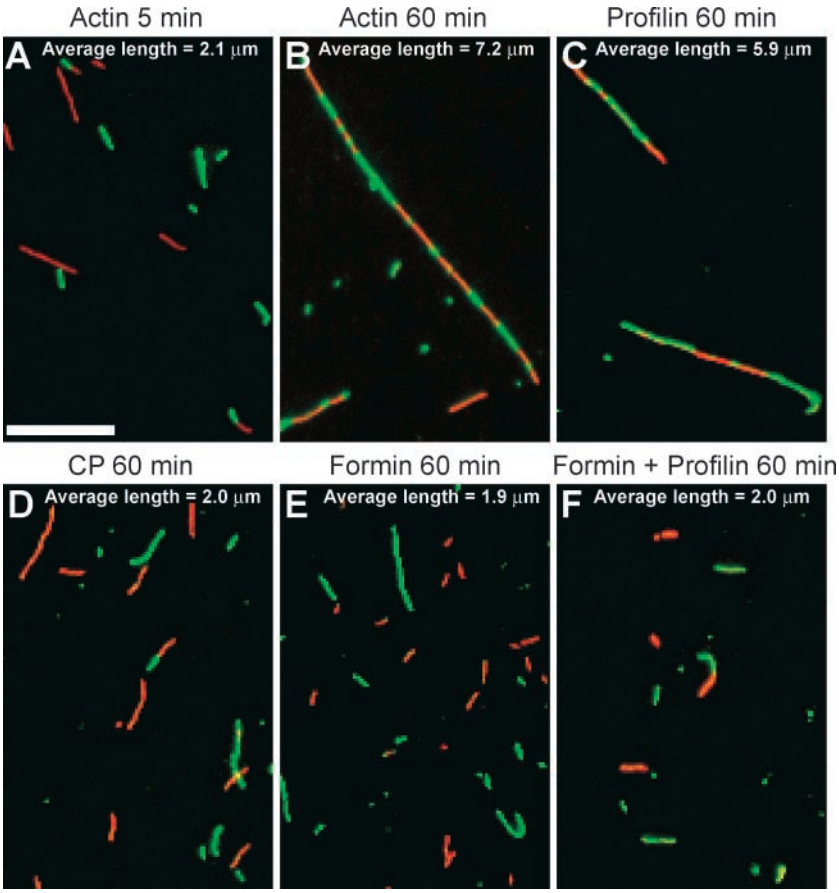

Figure 6. **Effects of Cdc12(FH1FH2)p and profilin on actin filament annealing.** Merged micrographs of red and green fluorescence. The buffer used was the same as in Fig. 2. Equal concentrations (0.25 μM) of red (rhodamine-phalloidin)- and green (Alexa® green–phalloidin)-labeled actin filaments were mixed, sheared through a 26-gauge needle, and allowed to anneal for up to 60 min before dilution and absorption to a coverslip coated with poly-L-lysine. Bar, 10 μm. (A) Actin filaments alone allowed to anneal for 5 min. (B) Actin filaments alone allowed to anneal for 60 min. (C) Actin filaments with 5 μM profilin after 60 min. (D) Actin filaments with 400 nM CP after 60 min. (E) Actin filaments with 400 nM Cdc12(FH1FH2)p after 60 min. (F) Actin filaments with 400 nM Cdc12(FH1FH2)p and 5 μM profilin after 60 min.

(FH1FH2)p and profilin grew at only one end at a rate characteristic of barbed ends (Fig. 5, H and I). Owing to the high concentration of filaments and their rapid growth, these samples depleted the actin monomer concentration with an exponential time course and a half time of 202 ± 88 s, such that they were growing at less than their maximum rate when first observed 100 s after initiation of polymerization. By extrapolation, we calculated the average initial rate to be 12.4 ± 5.9/s, similar to the rate of growth at barbed ends of actin alone, 16.2 ± 0.1/s, or actin plus profilin, 16.6 ± 0.1/s. The low concentrations of filaments in these control samples did not deplete the subunit pool, so they were growing at their maximum rate when first observed and continuously thereafter for >900 s. Extrapolation of the exponential time courses for actin with Cdc12(FH1FH2)p and profilin to zero length showed that most filaments began growing soon after initiating the reaction. Variations in the time of nucleation or annealing (rather than intermittent or variable rates of elongation) account for the variations in length observed at the end of the reaction. The combination of Cdc12(FH1FH2)p and profilin-Y5D, with affinity for poly-L-proline reduced 100-fold (Lu and Pollard, 2001), prevented both barbed and pointed end filament growth (unpublished data).

To learn if profilin dissociates Cdc12(FH1FH2)p from the barbed ends of filaments, we tested the effects of Cdc12(FH1FH2)p and profilin on the annealing of preformed filaments (Fig. 6). We sheared a mixture of 0.25 μM red (rhodamine-phalloidin)- and green (Alexa®488-phalloidin)-labeled actin filaments and followed annealing by fluorescence microscopy for up to 60 min (Andrianantoandro et al., 2001). 5 min after shearing, the actin filaments averaged 2.1 μm in length with 0.075 annealing red/green events per filament (Fig. 6 A). After 60 min, actin filaments averaged 7.2 μm in length with an average of 2.1 red/green annealing events per filament (Fig. 6 B). This assay underestimates annealing because it does not detect red/red or green/green annealing events. 5 μM profilin inhibited annealing modestly, with an average filament length of 5.9 μm with 1.2 red/green annealing events per filament after 60 min (Fig. 6 C), perhaps due to association with the barbed ends of actin filaments (Pollard and Cooper, 1984). Annealing was strongly inhibited by 400 nM capping protein (Fig. 6 D), 400 nM Cdc12(FH1FH2)p alone (Fig. 6 E), or 400 nM Cdc12 (FH1FH2)p with 5 μM profilin (Fig. 6 F), all yielding filaments ~2 μm long with <0.02 annealing events per filament 60 min after shearing. As little as 25 nM Cdc12 (FH1FH2)p inhibited annealing to the same extent as 400 nM Cdc12(FH1FH2)p, and a range of profilin concentrations (100 nM–5 μM) did not overcome this inhibition. Therefore, profilin appears to allow barbed end growth without removing formin.

Experiments on bulk samples confirmed that profilin allows actin filaments to elongate at their barbed ends in the presence of Cdc12(FH1FH2)p. Profilin inhibited the ability of Cdc12(FH1FH2)p to shift the critical concentration for actin assembly from that of the barbed end to that of the pointed end (Fig. 7 A). In the presence of 5 μM profilin,

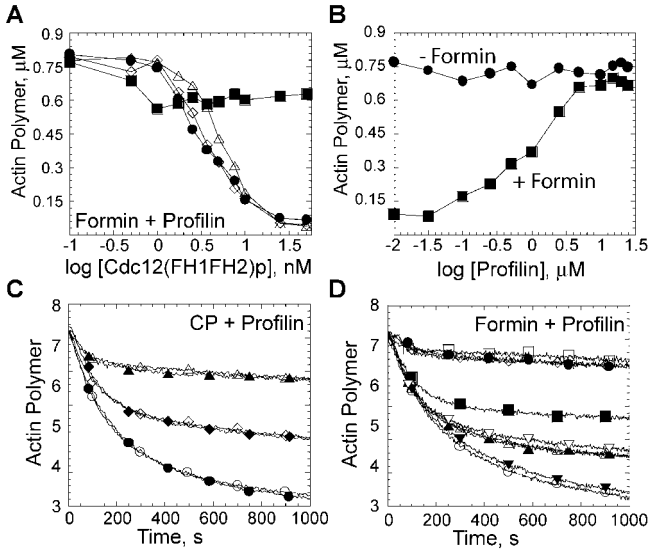

Figure 7. **Profilin inhibits capping of actin filament barbed ends by Cdc12(FH1FH2)p.** The buffer used was the same as in Fig. 2. (A and B) Dependence of the polymerization of 1 μM actin on the concentration of Cdc12(FH1FH2)p and on the presence of profilin. 5 μM polymerized actin (10% pyrene labeled) was diluted to 1 μM in the presence of either (A) a range of Cdc12(FH1FH2)p concentrations and 5 μM profilin or (B) a range of profilin concentrations and 50 nM Cdc12(FH1FH2)p. After 16 h, the actin polymer concentration was measured by pyrene fluorescence. (A) Dependence of actin polymer concentration on the concentration of Cdc12(FH1FH2)p either (●) alone or Cdc12(FH1FH2)p with (■) 5 μM wild-type profilin, (◇) 5 μM profilin-Y5D, or (△) 5 μM profilin-K81E. (B) Dependence of actin polymer concentration on the concentration of profilin in either the (●) absence or (■) presence of 50 nM Cdc12(FH1FH2)p. (C and D) Time course of the depolymerization of 5 μM actin filaments (70% pyrene labeled) after dilution to 0.1 μM. (C) Depolymerization of (○) actin alone or actin in the presence of (●) 5 μM wild-type profilin, (◇) 1 nM *Mm*CP, (◆) 1 nM *Mm*CP + 5 μM wild-type profilin, (△) 5 nM *Mm*CP, or (▲) 5 nM *Mm*CP + 5 μM wild-type profilin. (D) Depolymerization of (○) actin alone or actin in the presence of (▲) 2 nM Cdc12(FH1FH2)p, (▼) 2 nM Cdc12(FH1FH2)p + 5 μM wild-type profilin, (△) 2 nM Cdc12(FH1FH2)p + 5 μM profilin-Y5D, (▽) 2 nM Cdc12(FH1FH2)p + 5 μM profilin-K81E, (●) 10 nM Cdc12(FH1FH2)p, (■) 10 nM Cdc12(FH1FH2)p + 5 μM wild-type profilin, (◇) 10 nM Cdc12(FH1FH2)p + 5 μM profilin-Y5D, or (□) 10 nM Cdc12(FH1FH2)p + 5 μM profilin-K81E.

Cdc12(FH1FH2)p concentrations up to 0.1 μM reduced the actin polymer concentration to only slightly less than actin alone (Fig. 7 A); thus the effect on the critical concentration was minimal. The concentration of profilin determined its ability to inhibit the shift in the critical concentration caused by Cdc12(FH1FH2)p (Fig. 7 B), consistent with a low micromolar K_d for profilin and formin. Profilins lacking affinity for either actin monomers (profilin-K81E) or the formin FH1 domain (profilin-Y5D) did not inhibit barbed end capping by Cdc12(FH1FH2)p (Fig. 7 A).

A depolymerization experiment addressed whether profilin allows subunits to dissociate from barbed ends in the presence of Cdc12(FH1FH2)p (Fig. 7, C and D). Profilin prevented Cdc12(FH1FH2)p (Fig. 7 D) but not *Mm*CP (Fig. 7 C) from reducing the depolymerization rate of actin filaments diluted to 0.1 μM. This effect required profilin binding to both actin and poly-L-proline (Fig. 7 D). Thus, profilin allows subunit addition and loss at barbed ends saturated with Cdc12(FH1FH2)p.

Effect of profilin on spontaneous actin assembly in the presence of Cdc12(FH1FH2)p

Profilin had opposite effects on spontaneous polymerization of Mg-ATP actin monomers in the presence of Cdc12 (FH1FH2)p and capping protein. Like other profilins, wild-type fission yeast profilin inhibited spontaneous polymerization of actin (Lu and Pollard, 2001) and polymerization initiated by capping protein (Fig. 8, A and C). However, in the presence of 25 nM Cdc12(FH1FH2)p (Fig. 8, A and B), concentrations of profilin up to 5 μM reduced the initial lag at the outset of polymerization and increased the rate of polymer formation.

The calculation of filament ends revealed that profilin inhibited nucleation by Cdc12(FH1FH2)p, and that this stimulation of polymerization by profilin was due solely to enhancing the rate of elongation. Given that profilin allows barbed end growth (Fig. 5), the polymerization rates correspond to a maximum yield of only 0.015 barbed ends per formin polypeptide. In the absence of profilin, 25 nM Cdc12(FH1FH2)p yielded 0.09 pointed ends per formin polypeptide (Fig. 4). This sixfold reduction in nucleation by profilin can be attributed to the inhibition of both spontaneous and Cdc12(FH1FH2)p-mediated nucleation as well as depletion of the actin monomer pool by rapid elongation at the barbed ends that were created. Concentrations of wild-type profilin >5 μM reduced nucleation by 25 nM Cdc12(FH1FH2)p even further (Fig. 8 B). Consistent with barbed end growth, wild-type profilin lowered the monomer concentration required for spontaneous assembly with Cdc12(FH1FH2)p (Fig. 8 D).

The ability of profilin to promote spontaneous polymerization by Cdc12(FH1FH2)p required that the profilin have affinity for both actin monomers and proline-rich sequences (FH1 domain). Profilin-K81E lacking affinity for actin had no effect on polymerization with Cdc12(FH1FH2)p (Fig. 8 A). Profilin-Y5D lacking affinity for poly-L-proline inhibited spontaneous assembly of actin in both the absence and presence of Cdc12(FH1FH2)p (Fig. 8, A and B). Wild-type profilin and profilin-Y5D inhibited polymerization with *Mm*CP (Fig. 8 C).

Fluorescence microscopy of the products of these polymerization reactions confirmed that profilin allows Cdc12 (FH1FH2)p to nucleate a modest number of longer filaments. We stopped the reactions and labeled the filaments with rhodamine-phalloidin (Fig. 8, E–H) 600 s after initiating polymerization (Fig. 8 A). The number average lengths of filaments were 22.3 μm for 4 μM Mg-ATP actin alone (Fig. 8 E), 19.7 μm for 4 μM Mg-ATP actin with 5 μM profilin (Fig. 8 F), 1.0 μm for 4 μM Mg-ATP actin with 100 nM Cdc12(FH1FH2)p (Fig. 8 G), and 3.5 μm for 4 μM Mg-ATP actin with 100 nM Cdc12(FH1FH2)p and 5 μM profilin (Fig. 8 H). We calculated the number concentration of filaments by dividing the polymer concentration by the average filament length (in subunits). The number of filaments formed with Cdc12(FH1FH2)p was approximately threefold less in the presence of profilin. 5

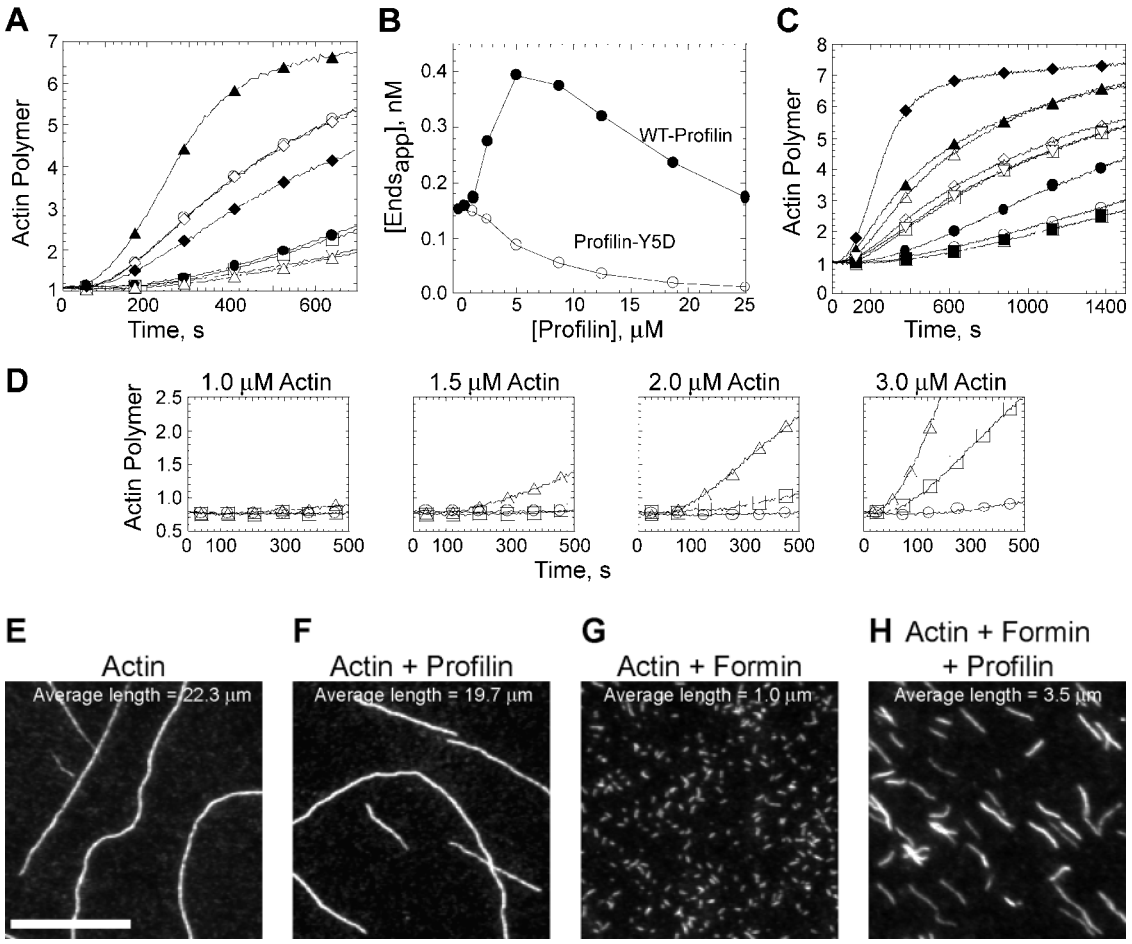

Figure 8. **Effect of profilin on spontaneous polymerization of Mg-ATP muscle actin in the presence of Cdc12(FH1FH2)p or mouse capping protein.** The buffer used was the same as in Fig. 2. (A) Time course of the polymerization of 4 μM Mg-ATP actin (2% pyrene labeled) in the presence of Cdc12(FH1FH2)p and either wild-type or mutant profilins; (□) 4 μM Mg-ATP actin alone or with (○) 25 nM Cdc12(FH1FH2)p, (▽) 5 μM wild-type profilin, (●) 5 μM profilin-K81E with a reduced affinity for actin, (△) 5 μM profilin-Y5D with a reduced affinity for poly-L-proline, (▲) 25 nM Cdc12(FH1FH2)p and 5 μM wild-type profilin, (◇) 25 nM Cdc12(FH1FH2)p and 5 μM profilin-K81E, or (◆) 25 nM Cdc12(FH1FH2)p and 5 μM profilin-Y5D. (B) Dependence of the concentration of ends produced by 4 μM Mg-ATP actin and 25 nM Cdc12(FH1FH2), as a function of the concentration of either (●) wild-type profilin or (○) profilin-Y5D. [Ends$_{app}$] was calculated at the time when 40% (1.6 μM) of the actin was polymerized, assuming barbed end growth. (C) Effect of profilin on capping protein nucleation. Time course of the polymerization of (●) 4 μM Mg-ATP actin alone or in the presence of (○) 5 μM wild-type profilin, (■) 5 μM profilin-Y5D, (△) 25 nM Cdc12(FH1FH2)p, (▲) 12.5 nM *Mm*CP, (◆) 25 nM Cdc12(FH1FH2)p and 5 μM wild-type profilin, (□) 25 nM Cdc12(FH1FH2)p and 5 μM profilin-Y5D, (◇) 12.5 nM *Mm*CP and 5 μM wild-type profilin, or (▽) 12.5 nM *Mm*CP and 5 μM profilin-Y5D. (D) Time course of the polymerization of the indicated concentrations of Mg-ATP actin alone (○) or with 25 nM Cdc12(FH1FH2)p alone (□), or with 25 nM Cdc12(FH1FH2)p and 5 μM wild-type profilin (△). Profilin lowered the concentration of actin monomer required for Cdc12(FH1FH2)p to stimulate polymerization. (E–H) Fluorescence micrographs of actin filaments labeled with rhodamine-phalloidin and adsorbed to glass coverslips coated with poly-L-lysine. Bar, 10 μm. (E) 4 μM Mg-ATP actin assembled alone. (F) Actin assembled with 5 μM wild-type profilin. (G) Actin assembled with 100 nM Cdc12(FH1FH2)p. (H) Actin assembled with 100 nM Cdc12(FH1FH2)p and 5 μM wild-type profilin.

μM wild-type profilin increased the average filament length by at least threefold at every Cdc12(FH1FH2)p concentration tested (25–250 nM). Neither profilin-K81E nor profilin-Y5D changed the length of 4 μM Mg-ATP actin with 100 nM Cdc12(FH1FH2)p (unpublished data).

Discussion

Our data on fission yeast Cdc12(FH1FH2)p agree in general with the findings of Pruyne et al. (2002), Sagot et al. (2002b), and Pring et al. (2003) on budding yeast Bni1(FH1FH2)p, so we think that both formins have similar mechanisms of action. The expression of constructs consisting of formin FH1 and FH2 domains at least partially complements the loss of formin function in both budding yeast (Sagot et al., 2002b) and fission yeast (this paper). Overexpression of (FH1FH2)p is lethal and dramatically increases actin cables in both yeast (Pruyne et al., 2002; Sagot et al., 2002b; this paper). In vitro, purified formin (FH1FH2)p constructs from both yeast stimulate the spontaneous assembly of actin filaments. Low concentrations of wild-type profilin enhance formin-induced polymerization, whereas higher concentrations inhibit actin polymerization (Sagot et al., 2002b; Pring et al., 2003; this paper). The ability of profilin to enhance actin polymerization by formins requires that the profilin binds both actin monomers and

the proline-rich FH1 domain (Sagot et al., 2002b; Pring et al., 2003; this paper). Although these data agree, additional evidence presented here revealed a mechanism of formin action different than proposed earlier.

We find that Cdc12(FH1FH2)p alone caps actin filament barbed ends and nucleates new filaments that grow exclusively from their pointed end. Profilin completely changes the reaction by inhibiting nucleation, uncapping barbed ends, and allowing formin-nucleated filaments to grow exclusively from their barbed ends (see Fig. S1, available at http://www.jcb.org/cgi/content/full/jcb.200211078/DC1). These insights explain why profilin is necessary in vivo for formin-dependent assembly of contractile rings and actin cables but is not required in vitro for formin-driven actin polymerization.

Formins cap the barbed end of actin filaments

Sagot et al. (2002b) and Pruyne et al. (2002) concluded that FH1FH2 constructs alone nucleate filaments that grow from their barbed ends. This interpretation was based on the ability of cytochalasins to inhibit polymerization stimulated by formin or spectrin–actin seeds, but not polymerization by the barbed end capping protein gelsolin. These investigators assumed that cytochalasins only inhibit growth at barbed ends, but the concentrations used inhibit elongation at both ends (Sampath and Pollard, 1991). Consequently, inhibition by cytochalasin is not a decisive test for the direction of growth. It is not clear to us why 2 μM cytochalasin B failed to inhibit growth from gelsolin nuclei (Pruyne et al., 2002). On the other hand, Bni1(FH1FH2)p was found to bind near the barbed ends of actin filaments and slowed barbed end assembly and disassembly by 50%, suggesting that Bni1(FH1FH2)p partially caps barbed ends (Pruyne et al., 2002; Pring et al., 2003). Direct experimental comparison is required to determine what differences, if any, exist between fission and budding yeast formin constructs.

All of our evidence is consistent with formin(FH1FH2)p constructs functioning like classic barbed end capping proteins that prevent subunit loss and addition at the barbed end and shift the critical concentration for assembly to that of the pointed end. Like capping protein, Cdc12 (FH1FH2)p nucleates filaments that grow exclusively from their pointed ends. Accordingly, formins may promote actin nucleation either by resembling an actin dimer or by capturing actin monomers or dimers like capping protein (Cooper and Pollard, 1985; Caldwell et al., 1989).

The available evidence suggests interesting similarities and differences between formins and capping protein. Given sufficient actin monomers, both proteins initiate numerous pointed ends. Although each filament grows slowly, their abundance rapidly consumes the available actin subunits. Because nucleation reactions depend strongly on the concentration of actin monomer, the rate of nucleation by formin and capping protein falls rapidly during a reaction and the concentration of ends peaked under our conditions when only 30% of the subunits were assembled. In contrast, Arp2/3 complex makes new filaments until nearly all of the subunits are consumed (Higgs et al., 1999). The maximum yield of new ends per initiator protein is achieved at very low concentrations of formin and capping protein, as higher concentrations accelerate depletion of the subunit pool. Although similar in many ways, capping protein caps barbed ends faster than formin. In TIRF experiments, the small number of barbed ends that formed spontaneously grew longer in the presence of 250 nM Cdc12(FH1FH2)p than in the presence of 50 nM capping protein. Capping protein capped most of the barbed ends during the ~90 s required to initiate observations, whereas formin capping continued over 10 min.

Given the functional similarities, we considered whether formin FH2 domains might be folded like capping protein. Capping proteins are heterodimers of α and β subunits having the same fold (Yamashita et al., 2003) but sharing only 30% conserved (identical plus similar) residues. The genes for α and β subunits have diverged not only from each other but also between species, as evolutionarily distant α subunits are conserved at only ~45% of the residue positions and distant β subunits are conserved at only ~60% of positions. Genes coding formin FH2 domains have also diverged considerably between and within species, being conserved at only ~40% of residue positions between evolutionarily distant species. We note that FH2 domains and capping protein subunits are approximately the same size and that the amino acid sequences can be aligned with few gaps (see Figs. S2 and S3, available at http://www.jcb.org/cgi/content/full/jcb.200211078/DC1). In these alignments, FH2 domain residues are conserved relative to evolutionarily distant capping protein α subunits at ~23% of the positions and with β subunits at ~22% of the positions. Within a given species, FH2 domain residues are conserved relative to their own capping protein α subunits at ~21% of positions and with β subunits at ~22% of positions. In the chicken capping protein structure, 37 residues are structurally conserved between the α and β subunits (Yamashita et al., 2003). About 65% of these structurally conserved residues are also conserved in the fission yeast capping protein subunits, and ~40% of the corresponding residues are conserved in FH2 domains (43% for Cdc12(FH2)p and 38% for mDIA (FH2)p). Given the structural similarity of the divergent α and β capping protein subunits and the presence of conserved residues between both capping protein subunits and FH2 domains, it is possible that two FH2 domains form a homodimeric capping protein. Further work is required to establish the extent, if any, of the structural homology between capping proteins and formin FH2 domains.

Profilin gates barbed end capping by formins

Our evidence shows that formins are a special type of capping protein that are gated by profilin. Formins cap the barbed end of actin filaments in the absence, but not in the presence, of profilin. As actin bound to profilin does not elongate pointed ends (Pollard and Cooper, 1984; Kaiser et al., 1999; confirmed here in Fig. 5), and capping protein blocks barbed ends, profilin inhibits actin assembly in the presence of capping protein (Fig. 8 C). Quite to the contrary, profilin promotes spontaneous assembly of actin in the presence of Cdc12(FH1FH2)p (Fig. 8 C). In principle, profilin might increase either the efficiency of nucleation by formin (Sagot et al., 2002b) or the rate of elongation after nucleation.

TIRF microscopy revealed that profilin reverses the polarity of actin filament assembly driven by Cdc12(FH1FH2)p (Fig. 5), so the filaments grow exclusively at their fast growing barbed end with profilin and exclusively at their pointed ends without profilin. Given that each filament grows at least 15 times faster with profilin, and that the bulk polymerization rate is only slightly faster with profilin than with Cdc12(FH1FH2)p alone (Fig. 8 A), profilin must inhibit nucleation by up to sixfold. Accordingly, filaments were at least three times longer with profilin and Cdc12(FH1FH2)p than with Cdc12(FH1FH2)p alone (Fig. 8, E–H), indicating the production of at least threefold fewer filaments. Profilin also inhibits nucleation by budding yeast formin Bni1(FH1FH2)p (Pring et al., 2003). Two mechanistic questions arise.

First, how does profilin inhibit nucleation by formins? The simplest hypothesis is that formins utilize spontaneously formed actin dimers to form nuclei for pointed end growth. Profilin inhibits spontaneous actin nucleation, most likely the formation of dimers (Pollard and Cooper, 1984). Lacking these spontaneously assembled actin dimers, formin cannot start new filaments. More complicated mechanisms are possible, particularly because profilin must bind both FH1 and actin for its positive effects on assembly, whereas profilin lacking affinity for polyproline merely inhibits assembly. Thus, nucleation by profilin plus formin may involve a ternary complex that has yet to be characterized.

Second, how does profilin reverse the direction of actin elongation in the presence of formin? Explaining the lack of growth at the point end is simple, because an actin monomer with profilin bound to its barbed end cannot elongate the pointed end of an actin filament (Pollard and Cooper, 1984). The mechanism allowing elongation at the barbed end in the presence of formin is less clear. Most simply, profilin might dissociate formin from the barbed end. However, Cdc12(FH1FH2)p inhibits annealing even in the presence of profilin (Fig. 6), suggesting that formins remain associated with barbed ends. We suspect that bivalent binding of profilins to actin and FH1 contributes to opening the cap at the barbed end while blocking annealing, but the details remain to be discovered. Doping annealing reactions with additional actin monomers did not allow profilin to overcome Cdc12(FH1FH2)p inhibition of annealing (unpublished data). Thus, profilin may allow barbed end elongation with the profilin–formin complex surfing at or near the barbed end like microtubule end binding proteins (for review see Howard and Hyman, 2003).

Assembly of actin cables and contractile rings

Formins and profilin are both implicated in contractile ring assembly in diverse organisms (Balasubramanian et al., 1994; Haugwitz et al., 1994; Verheyen and Cooley, 1994; Chang et al., 1997; Severson et al., 2002; Tolliday et al., 2002) and actin cables in yeast (Feierbach and Chang, 2001b; Evangelista et al., 2002; Sagot et al., 2002a). Temperature-sensitive mutants of fission yeast profilin (*cdc3-313*) and Cdc12p (*cdc12-112*) have synthetic lethal genetic interactions, and profilin binds the proline-rich formin(FH1)p domain (Chang et al., 1997; Wasserman, 1998). This argues that the two proteins operate on the same pathway, mostly likely through direct interaction.

All of the available biochemical and biological evidence suggests that formins and profilin cooperate to assemble actin filaments for contractile rings and cables. Localization of formins to the equator of mitotic cells before assembly of a contractile ring and to the buds before cable formation places them at the site of actin assembly. Given the abundance of profilin in most cells, the most likely mechanism is that formins overcome the inhibition of spontaneous nucleation by profilin and generate filaments that grow in the barbed direction. Many details remain to be resolved. In particular, we must still learn how formins can remain near the barbed ends of filaments (for example in buds; Ozaki-Kuroda et al., 2001) as the filaments grow and whether contractile rings and cables consist of short overlapping filaments or long filaments.

Given the opposite effects of profilin on actin filaments capped by Cdc12(FH1FH2)p and capping protein in vitro, it is likely that formins and capping protein compete for actin filament barbed ends in vivo. Consistent with this hypothesis, the overexpression of capping protein in fission yeast causes a specific lethal defect in cytokinesis, and capping protein and *cdc12* have an antagonistic genetic relationship (unpublished data). It will be of considerable interest to understand how cells regulate the balance between capping protein– and formin-capped barbed ends depending on the necessity for rapid filament assembly.

Materials and methods

Strains, media, and electroporation

Wild-type *S. pombe* strain *FY436* (KV25; *h⁻ his7-366 ura4-D18 leu1-32 ade6-M216*) and temperature-sensitive strain *cdc12-112* (KV145; *h⁺ ade6-M210 ura4-D18 Leu1-32*; Chang et al., 1997) were used in this study. We used standard growth media (YES rich medium and EMM minimal medium) and methods for electroporation and molecular biology (Sambrook et al., 1989; Moreno et al., 1991; Wu et al., 2001). Expression under the *nmt1* promoter was regulated in EMM medium with the presence or absence of 10.0 μg/ml thiamine (Sigma-Aldrich).

Plasmid construction

A region of *cdc12* containing the FH1 and FH2 domains (residues 882–1375) was amplified from genomic DNA by high fidelity PCR (Pfu; Stratagene) and cloned into the vectors *pGEX-4T* (Amersham Biosciences) for expression in *Escherichia coli* and *pREP41* (Maundrell, 1990) for expression in *S. pombe*. Inserts of the recombinant plasmids (*pGEX-cdc12[FH1FH2]* and *pREP41-cdc12[FH1FH2]*) were sequenced to confirm fidelity of the PCR amplification.

Microscopy of cells

Cell morphology was observed by differential interference contrast (DIC) and epifluorescence microscopy. Images were collected with a cooled CCD camera (Orca-ER; Hamamatsu) on an Olympus IX71 microscope with a 60X 1.4 NA Plan-apo objective. Nuclei and septa were stained by adding 0.1 volume of a 1 mg/ml stock (in water) of Hoechst (bisBenzimide; Sigma-Aldrich) for 30 min. *S. pombe* were fixed for 2 min with 0.1 volume of 16% formaldehyde (Electron Microscopy Sciences) and permeabilized for 30 s with 1% Nonidet P-40 (Sigma-Aldrich), and filamentous actin was stained with 7.5 μg/ml rhodamine-phalloidin (Fluka) in DAPI mounting medium (50% glycerol containing 1 mg/ml *p*-phenylelediamine [Sigma-Aldrich] and 1 μg/ml DAPI [Sigma-Aldrich] in PBS) for at least 6 h. We quantitated the effects of Cdc12(FH1FH2)p overexpression using at least two transformed strains analyzed on separate days. At least 300 cells were counted for each point. The culture density was kept between 0.1 and 0.5 (OD_{595}) throughout the time course. We measured cell density, nuclei per cell (DAPI), septal morphology (Calcoflour, 1 mg/ml in water), and the presence of actomyosin rings (pREP42-GFP–*cdc4*; Balasubramanian et al., 1997).

Protein purification

Recombinant Cdc12(FH1FH2)p was purified from the GST fusion protein construct similar to budding yeast Bni1p (Pruyne et al., 2002). The *pGEX-4T-Cdc12(FH1FH2)* construct was transformed into *E. coli* strain BL21-Codon Plus (DE3)-RP (Stratagene) and grown overnight at 37°C. After subculturing into fresh media, cells were grown at 30°C for 3 h and then induced for 24 h at 16°C with the addition of 0.5 mM isopropyl β-D-thiogalactopyranoside. Cells harvested by centrifugation were frozen, resuspended in extraction buffer (20 mM Hepes, pH 7.4, 200 mM NaCl, 10% glycerol, and 5 mM DTT) supplemented with a complete protease inhibitor tablet (Roche), and sonicated. The sonicate was clarified at 30,000 and 50,000 *g* for 20 min each and loaded onto a 1.5 ml glutathione-Sepharose column (Amersham Biosciences). After the column was washed with 15 bed volumes of wash buffer (20 mM Hepes, pH 7.4, 200 mM NaCl, 10% glycerol, and 1 mM DTT), an additional 1 ml of wash buffer, supplemented with 50 U of thrombin (Amersham Biosciences), was added and incubated on a rocker for 16 h at 4°C. Thrombin-cleaved Cdc12(FH1FH2)p was collected and dialyzed against Source Q-buffer (20 mM Tris, pH 8.5, 25 mM NaCl, 1 mM DTT, 5% glycerol, and 0.01% NaN_3) for 24 h at 4°C. Dialyzed protein was loaded onto a 1-ml Source 15Q column (Amersham Biosciences), washed with two column volumes, and then eluted with a 75-ml linear gradient of 25–500 mM NaCl in Source Q-buffer. Pure Cdc12(FH1FH2)p was dialyzed into buffer P (20 mM Hepes, pH 7.4, 1 mM EDTA, 50 mM KCl, 5% glycerol, 1 mM DTT, 0.01% NaN_3). When stored on ice, Cdc12(FH1FH2)p aggregated slowly and lost activity (half life for activity was ~2 wk). The activity of Cdc12(FH1FH2)p flash frozen in liquid nitrogen and stored at −80°C appeared indistinguishable from freshly purified protein. Therefore, we used freshly purified protein stored on ice (within 1 wk) or protein stored at −80°C (within 1 wk after thawing) for all experiments. Three independent batches of Cdc12(FH1FH2)p gave similar results.

Mouse capping protein α1 and β2 subunits (*Mm*CP) was purified from bacteria (Palmgren et al., 2001). Wild-type and Y5D and K81E mutant *S. pombe* profilins were purified from bacteria (Lu and Pollard, 2001). Ca-ATP actin was purified from rabbit skeletal muscle (Spudich and Watt, 1971) and gel filtered on Sephacryl S-300 in G buffer (2 mM Tris, pH 8.0, 0.2 mM ATP, 0.1 mM $CaCl_2$, and 0.5 mM DTT) to remove capping protein and oligomers. Actin was labeled on Cys-374 with either pyrenyliodoacetamide (Molecular Probes) (Pollard, 1984) or a 12-fold excess of Oregon green 488 iodoacetamide (Molecular Probes). Actin was depolymerized by dialysis against two changes of G buffer. Oregon green actin (Ca-OG-actin) was further purified by anion exchange chromatography on DE52 (Whatman) in G buffer with 5 mM Pipes-Tris, pH 6.5, and eluted with a linear gradient of 0–300 mM KCl. Peak fractions were polymerized by dialysis overnight against 5 mM imidazole, pH 7.5, 100 mM KCl, 2 mM $MgSO_4$, 0.5 mM EGTA, 0.3 mM ATP, 0.5 mM DTT, and 1 mM NaN_3. The final purification step for both labeled actins was depolymerization by dialysis against G buffer and gel filtration on Sephacryl S-300.

Protein concentrations were determined with extinction coefficients as follows: unlabeled actin, A_{290} = 26,600 M^{-1} cm^{-1} (Houk and Ue, 1974); pyrene-actin, (A_{290} − [A_{344} × 0.127]) × 38.5 μM (Cooper et al., 1983); Oregon green actin, [Total Ca-actin] = (A_{290} − [A_{491} × 0.16991])/26,600 M^{-1} cm^{-1}, [Ca-OG-actin] = A_{491}/77,800 M^{-1} cm^{-1}; wild-type and mutant profilin, A_{280} = 1.63 OD mg^{-1} ml^{-1} (Lu and Pollard, 2001); and *Mm*CP, A_{280} = 76.3 mM^{-1} cm^{-1} (Palmgren et al., 2001). An extinction coefficient (A_{280}) of 49,860 M^{-1} cm^{-1} for Cdc12(FH1FH2)p was estimated with ProtParam (http://us.expasy.org/tools/) from the amino acid composition.

Fluorescence spectroscopy

The concentration of polymerized actin was measured from the fluorescence of a trace of pyrene-actin (excitation at 365 nm and emission at 407 nm) with a PTI Alphascan spectroflourimeter (Photon Technology International) (Higgs et al., 1999). For spontaneous polymerization assays, pyrene-labeled and unlabeled Ca-ATP actin monomers were mixed in G buffer to obtain a 20 μM stock solution of either 5% pyrene-actin or 2% pyrene-actin for experiments with profilin. An aliquot of stock was converted to Mg-ATP actin by adding 0.1 volume of 10 mM EGTA and 1 mM $MgCl_2$ for 2 min at 25°C. Separate drops of Mg-ATP actin, other proteins, and 10× KMEI (500 mM KCl, 10 mM $MgCl_2$, 10 mM EGTA, and 100 mM imidazole, pH 7.0) were placed on the side of a plastic Eppendorf tube. The reaction was started by mixing with G buffer–Mg (G buffer with 0.1 mM $MgCl_2$ in place of 0.1 mM $CaCl_2$). For depolymerization assays (Caldwell et al., 1989), a 5 μM stock of 70% pyrene F-actin was prepared and diluted to 0.1 μM, in the presence of a range of concentrations of Cdc12(FH1FH2)p or *Mm*CP with or without 5 μM profilin, with the addition of F buffer (G buffer supplemented with 10× KMEI). The critical concentration for actin assembly was determined two ways. First, a range of concentrations of Mg-ATP actin (5% pyrene labeled) was polymerized in the absence or presence of either 10 nM *Mm*CP or 100 nM Cdc12(FH1FH2)p in F buffer for 16 h in the dark at 25°C. Second, a 5 μM stock of 10% pyrene F-actin was prepared and diluted to 1.0 μM with F buffer, in the presence of a range of concentrations of Cdc12(FH1FH2)p with or without 5 μM profilin (Caldwell et al., 1989). Reactions were incubated for at least 12 h in the dark at 25°C.

Calculation of the concentration of apparent ends, [$Ends_{app}$], and depolymerization rates

The concentration of apparent pointed ends, [$Ends_{app}$], was calculated from elongation rates using the equation [$Ends_{app}$] = elongation rate/(k_+[actin monomers]), where k_+ = 0.8 μM^{-1} s^{-1} at pH 7.0, as previously described (Higgs et al., 1999). As [$Ends_{app}$] peaked when about one third of the 4 μM G-actin had polymerized in the presence of Cdc12(FH1FH2)p and *Mm*CP (not depicted), we used the elongation rate at 2.4 μM G-actin to calculate [$Ends_{app}$]. In the presence of profilin, the concentration of apparent barbed ends, [$Ends_{app}$], was calculated where k_+ = 11.6 μM^{-1} s^{-1} at pH 7.0 (Pollard, 1986). The yield of [$Ends_{app}$] per capping molecule was calculated by dividing the [$Ends_{app}$] by the concentration of Cdc12(FH1FH2)p or *Mm*CP and subtracting the [$Ends_{app}$] for actin alone. The rate of depolymerization was calculated by fitting the data from 300–1,000 s with a single exponential curve. Depolymerization rates in the presence of Cdc12(FH1FH2)p or *Mm*CP were expressed as a percent normalized to the rate of actin alone.

Microscopy of rhodamine-phalloidin–labeled filaments

Products of polymerization were examined by fluorescence microscopy (Blanchoin et al., 2000). Actin filaments were removed from polymerization assays and labeled by diluting 3 μl of the reaction with 15 μl of 1 μM rhodamine-phalloidin (Fluka) in fluorescence buffer containing 50 mM KCl, 1 mM $MgCl_2$, 100 mM DTT, 20 μg/ml catalase, 100 μg/ml glucose oxidase, 3 mg/ml glucose, 0.5% methylcellulose, 10 mM imidazole, pH 7.0, for 5 min. After diluting with an additional 500 μl of fluorescence buffer, 2 μl was applied to coverslips coated with 0.05 μg/μL poly-L-lysine, and fluorescence images were collected with a cooled CCD camera (Orca-ER) on an Olympus 1X-71 microscope.

Actin filament annealing

Annealing (Andrianantoandro et al., 2001) was examined by polymerizing 4 μM Mg-ATP actin in the presence of either 6 μM rhodamine- or 6 μM Alexa® green–phalloidin (Molecular Probes) for 1 h. Equal volumes of red and green filaments (0.5 μM total final actin filament concentration) and *Mm*CP, Cdc12(FH1FH2)p, or profilin were mixed in F buffer, sheared by pushing eight times through a 3/8-inch 26-gauge needle on a 1.0-ml tuberculin syringe, and allowed to anneal for 60 min at room temperature. Reactions were terminated by a 250-fold dilution in fluorescence buffer, absorbed to coverslips coated with poly-L-lysine, and imaged as described above. The number of annealing events per filament was determined by dividing the total number of red and green transitions within a population of filaments by the total number of those filaments.

TIRF microscopy

TIRF microscopy was performed using the methods of Amann and Pollard (2001) using Oregon green–labeled Mg-ATP actin (25–30% labeled) as a tracer and 0.0002% of 0.2-μm crimson fluorescent beads (Molecular Probes) as autofocusing targets. Images were collected with a cooled CCD camera (Orca-ER) using custom software that automatically focused on fluorescent beads via epifluorescence and corrected time-lapse TIRF movies for drift. A maximum intensity projection revealed movement-constricted NEM-myosin attachment points of individual filaments that we used as fiducial marks to separate the barbed and pointed ends for length measurements. Filament lengths were calculated from 370 subunits/μm. Polymerization rates were estimated from plots of change in length versus change in time for the entire population of filaments using a robust-MM linear regression algorithm of S-Plus (Insightful Corp.).

To quantify total filament content, long filaments were traced and measured by hand. Hand-traced filaments were masked out of the image, a threshold was applied to the remaining pixels, and particle area, *A*, and perimeter, *P*, were scored. Particles with a circularity of $4\pi A/P^2 > 0.5$ were discarded, and the remaining particle lengths were calculated from

$$P/4 + \sqrt{(P/4)^2 - A}.$$

Online supplemental material

The supplemental material (available at http://www.jcb.org/cgi/content/full/jcb.200211078/DC1) contains figures showing a diagram of the model for the mechanism of nucleation by Cdc12(FH1FH2)p in the presence of profilin, and alignments of capping protein α and β subunits with FH2 domains.

We thank Martin Wear and John Cooper (Washington University, St. Louis, MO) for supplying the mouse capping protein expression plasmid and members of the Pollard lab for preparing actin, technical assistance, and helpful discussions.

This work was supported by National Institutes of Health (NIH) research grants GM-26338 and GM-26132 (to T.D. Pollard), an NIH postdoctoral fellowship (to D.R. Kovar), and a Burroughs Wellcome Fund Career Award at the Scientific Interface (to J.R. Kuhn).

Submitted: 19 November 2002
Revised: 24 April 2003
Accepted: 24 April 2003

References

Alberts, A.S. 2001. Identification of a carboxyl-terminal diaphanous-related formin homology protein autoregulatory domain. *J. Biol. Chem.* 276:2824–2830.

Amann, K.J., and T.D. Pollard. 2001. Direct real-time observation of actin filament branching mediated by Arp2/3 complex using total internal reflection fluorescence microscopy. *Proc. Natl. Acad. Sci. USA.* 98:15009–15013.

Andrianantoandro, E., L. Blanchoin, D. Sept, J.A. McCammon, and T.D. Pollard. 2001. Kinetic mechanism of end-to-end annealing of actin filaments. *J. Mol. Biol.* 312:721–730.

Balasubramanian, M.K., B.R. Hirani, J.D. Burke, and K.L. Gould. 1994. The *Schizosaccharomyces pombe* cdc3+ gene encodes a profilin essential for cytokinesis. *J. Cell Biol.* 125:1289–1301.

Balasubramanian, M.K., D. McCollum, and K.L. Gould. 1997. Cytokinesis in fission yeast *Schizosaccharomyces pombe. Methods Enzymol.* 283:494–506.

Blanchoin, L., K.J. Amann, H.N. Higgs, J.B. Marchand, D.A. Kaiser, and T.D. Pollard. 2000. Direct observation of dendritic actin filament networks nucleated by Arp2/3 complex and WASP/Scar proteins. *Nature.* 404:1007–1011.

Caldwell, J.E., S.G. Heiss, V. Mermall, and J.A. Cooper. 1989. Effects of CapZ, an actin capping protein of muscle, on the polymerization of actin. *Biochemistry.* 28:8506–8514.

Chang, F., D. Drubin, and P. Nurse. 1997. cdc12p, a protein required for cytokinesis in fission yeast, is a component of the cell division ring and interacts with profilin. *J. Cell Biol.* 137:169–182.

Cooper, J.A., and T.D. Pollard. 1985. Effect of capping protein on the kinetics of actin polymerization. *Biochemistry.* 24:793–799.

Cooper, J.A., S.B. Walker, and T.D. Pollard. 1983. Pyrene actin: documentation of the validity of a sensitive assay for actin polymerization. *J. Muscle Res. Cell Motil.* 4:253–262.

Evangelista, M., D. Pruyne, D.C. Amberg, C. Boone, and A. Bretscher. 2002. Formins direct Arp2/3-independent actin filament assembly to polarize cell growth in yeast. *Nat. Cell Biol.* 4:260–269.

Feierbach, B., and F. Chang. 2001a. Cytokinesis and the contractile ring in fission yeast. *Curr. Opin. Microbiol.* 4:713–719.

Feierbach, B., and F. Chang. 2001b. Roles of the fission yeast formin for3p in cell polarity, actin cable formation and symmetric cell division. *Curr. Biol.* 11: 1656–1665.

Frazier, J.A., and C.M. Field. 1997. Actin cytoskeleton: are FH proteins local organizers? *Curr. Biol.* 7:R414–R417.

Guertin, D.A., S. Trautmann, and D. McCollum. 2002. Cytokinesis in eukaryotes. *Microbiol. Mol. Biol. Rev.* 66:155–178.

Haugwitz, M., A.A. Noegel, J. Karakesisoglou, and M. Schleicher. 1994. *Dictyostelium* amoebae that lack G-actin-sequestering profilins show defects in F-actin content, cytokinesis, and development. *Cell.* 79:303–314.

Higgs, H.N., L. Blanchoin, and T.D. Pollard. 1999. Influence of the C terminus of Wiskott-Aldrich syndrome protein (WASp) and the Arp2/3 complex on actin polymerization. *Biochemistry.* 38:15212–15222.

Houk, T.W., Jr., and K. Ue. 1974. The measurement of actin concentration in solution: a comparison of methods. *Anal. Biochem.* 62:66–74.

Howard, J., and A.A. Hyman. 2003. Dynamics and mechanics of the microtubule plus end. *Nature.* 422:753–758.

Kaiser, D.A., V.K. Vinson, D.B. Murphy, and T.D. Pollard. 1999. Profilin is predominantly associated with monomeric actin in *Acanthamoeba*. *J. Cell Sci.* 112(Pt. 21):3779–3790.

Kang, F., D.L. Purich, and F.S. Southwick. 1999. Profilin promotes barbed-end actin filament assembly without lowering the critical concentration. *J. Biol. Chem.* 274:36963–36972.

Kinosian, H.J., L.A. Selden, L.C. Gershman, and J.E. Estes. 2002. Actin filament barbed end elongation with nonmuscle MgATP-actin and MgADP-actin in the presence of profilin. *Biochemistry.* 41:6734–6743.

Le Goff, X., S. Utzig, and V. Simanis. 1999. Controlling septation in fission yeast: finding the middle, and timing it right. *Curr. Genet.* 35:571–584.

Lu, J., and T.D. Pollard. 2001. Profilin binding to poly-L-proline and actin monomers along with ability to catalyze actin nucleotide exchange is required for viability of fission yeast. *Mol. Biol. Cell.* 12:1161–1175.

Maundrell, K. 1990. nmt1 of fission yeast. A highly transcribed gene completely repressed by thiamine. *J. Biol. Chem.* 265:10857–10864.

Moreno, S., A. Klar, and P. Nurse. 1991. Molecular genetic analysis of fission yeast *Schizosaccharomyces pombe*. *Methods Enzymol.* 194:795–823.

Nakano, K., J. Imai, R. Arai, E.A. Toh, Y. Matsui, and I. Mabuchi. 2002. The small GTPase Rho3 and the diaphanous/formin For3 function in polarized cell growth in fission yeast. *J. Cell Sci.* 115:4629–4639.

Ozaki-Kuroda, K., Y. Yamamoto, H. Nohara, M. Kinoshita, T. Fujiwara, K. Irie, and Y. Takai. 2001. Dynamic localization and function of Bni1p at the sites of directed growth in *Saccharomyces cerevisiae. Mol. Cell. Biol.* 21:827–839.

Palmgren, S., P.J. Ojala, M.A. Wear, J.A. Cooper, and P. Lappalainen. 2001. Interactions with PIP2, ADP-actin monomers, and capping protein regulate the activity and localization of yeast twinfilin. *J. Cell Biol.* 155:251–260.

Pelham, R.J., and F. Chang. 2002. Actin dynamics in the contractile ring during cytokinesis in fission yeast. *Nature.* 419:82–86.

Petersen, J., O. Nielsen, R. Egel, and I.M. Hagan. 1998. FH3, a domain found in formins, targets the fission yeast formin Fus1 to the projection tip during conjugation. *J. Cell Biol.* 141:1217–1228.

Pollard, T.D. 1984. Polymerization of ADP-actin. *J. Cell Biol.* 99:769–777.

Pollard, T.D. 1986. Rate constants for the reactions of ATP- and ADP-actin with the ends of actin filaments. *J. Cell Biol.* 103:2747–2754.

Pollard, T.D., and G.G. Borisy. 2003. Cellular motility driven by assembly and disassembly of actin filaments. *Cell.* 112:453–465.

Pollard, T.D., and J.A. Cooper. 1984. Quantitative analysis of the effect of *Acanthamoeba* profilin on actin filament nucleation and elongation. *Biochemistry.* 23:6631–6641.

Pring, M., M. Evangelista, C. Boone, C. Yang, and S.H. Zigmond. 2003. Mechanism of formin-induced nucleation of actin filaments. *Biochemistry.* 42:486–496.

Pruyne, D., M. Evangelista, C. Yang, E. Bi, S. Zigmond, A. Bretscher, and C. Boone. 2002. Role of formins in actin assembly: nucleation and barbed-end association. *Science.* 297:612–615.

Robinson, D.N., and J.A. Spudich. 2000. Towards a molecular understanding of cytokinesis. *Trends Cell Biol.* 10:228–237.

Sagot, I., S.K. Klee, and D. Pellman. 2002a. Yeast formins regulate cell polarity by controlling the assembly of actin cables. *Nat. Cell Biol.* 4:42–50.

Sagot, I., A.A. Rodal, J. Moseley, B.L. Goode, and D. Pellman. 2002b. An actin nucleation mechanism mediated by Bni1 and profilin. *Nat. Cell Biol.* 4:626–631.

Sambrook, J., E.F. Fritsch, and T. Maniatis. 1989. Molecular Cloning: A Laboratory Manual. Cold Spring Harbor Laboratory, Cold Spring Harbor, NY. 1.1–18.88.

Sampath, P., and T.D. Pollard. 1991. Effects of cytochalasin, phalloidin, and pH on the elongation of actin filaments. *Biochemistry.* 30:1973–1980.

Severson, A.F., D.L. Baillie, and B. Bowerman. 2002. A formin homology protein and a profilin are required for cytokinesis and Arp2/3-independent assembly of cortical microfilaments in *C. elegans. Curr. Biol.* 12:2066–2075.

Spudich, J.A., and S. Watt. 1971. The regulation of rabbit skeletal muscle contraction. I. Biochemical studies of the interaction of the tropomyosin-troponin complex with actin and the proteolytic fragments of myosin. *J. Biol. Chem.* 246:4866–4871.

Tolliday, N., L. VerPlank, and R. Li. 2002. Rho1 directs formin-mediated actin ring assembly during budding yeast cytokinesis. *Curr. Biol.* 12:1864–1870.

Verheyen, E.M., and L. Cooley. 1994. Profilin mutations disrupt multiple actin-dependent processes during *Drosophila* development. *Development.* 120: 717–728.

Wasserman, S. 1998. FH proteins as cytoskeletal organizers. *Trends Cell Biol.* 8:111–115.

Wu, J.Q., J. Bahler, and J.R. Pringle. 2001. Roles of a fimbrin and an α-actinin-like protein in fission yeast cell polarization and cytokinesis. *Mol. Biol. Cell.* 12:1061–1077.

Yamashita, A., A. Maeda, and K. Maeda. 2003. Crystal structure of CapZ: structural basis for actin filament barbed end capping. *EMBO J.* 22:1529–1538.